

# Ubiquitous Nature of Rate Retardation in Reversible Addition-Fragmentation Chain Transfer Polymerization

Kate G. E. Bradford,<sup>†</sup> Leilah M. Petit,<sup>†</sup> Richard Whitfield,<sup>§</sup> Athina Anastasaki,<sup>\*,§</sup> Christopher Barner-Kowollik,<sup>\*,||</sup> and Dominik Konkolewicz<sup>\*,†</sup>

<sup>†</sup>Department of Chemistry and Biochemistry, Miami University, Oxford, OH, 45056, United States

<sup>§</sup>Laboratory of Polymeric Materials, Department of Materials, ETH Zurich, Vladimir-Prelog-Weg 5, Zurich, Switzerland

<sup>||</sup>Centre for Materials Science, School of Chemistry and Physics, Queensland University of Technology (QUT), 2 George Street, Brisbane, Queensland 4000, Australia

**KEYWORDS** *Polymerization Control • Polymerization Rate • Reversible Deactivation Radical Polymerization • RDRP • Rate Retardation*

---

**ABSTRACT:** Reversible addition-fragmentation chain transfer (RAFT) polymerization is one of the most powerful reversible-deactivation radical polymerization (RDRP) processes. Rate retardation is prevalent in RAFT and occurs when polymerization rates deviate from ideal conventional radical polymerization kinetics. Herein, we explore beyond what was initially thought to be the culprit of rate retardation; dithiobenzoate chain transfer agents (CTA) with more active monomers (MAMs). Remarkably, polymerizations showed that rate retardation occurs in systems encompassing the use of trithiocarbonates and xanthates CTAs with varying monomeric activities. Both the simple slow fragmentation and intermediate radical termination models show that retardation of all these systems can be described by using a single relationship for a variety of monomer reactivity and CTAs, suggesting rate retardation is a universal phenomenon of varying severity, independent of CTA composition and monomeric activity level.

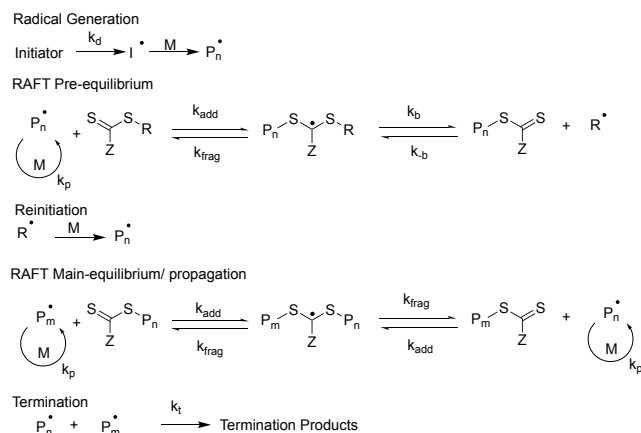
---

## INTRODUCTION

Polymers are macromolecules that are composed of chains of repeating units.<sup>1</sup> Polymers can be found everywhere in everyday life; from commodity plastics to medicine.<sup>2,3</sup> Their relative abundance in everyday life inspired macromolecular chemists to conceive polymerization methodologies that afford high levels of control over the chain length and distribution. Reversible addition-fragmentation chain transfer (RAFT) polymerization is a reversible deactivation radical polymerizations (RDRP) method that is known for its compatibility with many different monomers.<sup>4</sup> RAFT polymerization harnesses the use of chain transfer agents (CTAs) which gives it the ability to control molecular weight and provide narrow molecular weight distributions of polymer chains. RAFT polymerization can also be used to generate complex polymeric architecture, such as block, star, graft, branched, and network polymers, enabling a wide array of applications.<sup>5</sup>

Classical RAFT polymerization, shown in Scheme 1, undergoes thermal initiation to generate a radical species that subsequently react with monomer units to generate a propagating radical. This propagating radical can then enter into a pre-equilibrium stage with the CTA. The propagating radical adds to

thiocarbonylthio groups of the CTA to afford a RAFT intermediate radical, which can subsequently undergo fragmentation to release a new radical chain and give a dormant CTA capped polymer. This new radical is ideally able to add monomer units before adding to a CTA molecule. Once all small molecule CTA is converted to oligomeric CTAs, the chain transfer process can repeat itself in the main RAFT equilibrium as a propagating radical adds to a CTA molecule, transfers the radical to release another chain for controlled monomer addition. To obtain narrow molecular weight distributions, it is important that the addition is faster than propagation rate to encourage only a small amount of monomer addition per chain activation-deactivation cycle. In ideal RDRP, a typical activation-deactivation cycle may add zero or at most one monomer per cycle, as highlighted in models in the literature.<sup>6-9</sup> The process of activation-propagation-deactivation continues until all free monomer has been consumed, or until a nonproductive pathway occurs in which two radicals terminate.



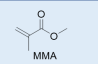
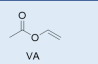
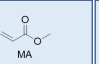
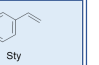
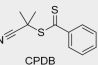
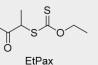
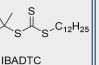
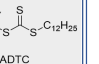
**Scheme 1:** Fundamental mechanism of RAFT polymerization.

RAFT polymerization is mediated by a variety of CTAs. These CTAs are (often) thiocarbonylthio compounds with varying R and Z groups. These R and Z groups must be adjusted for every monomer to ensure low dispersity and reasonable reaction rates. The four common types of CTAs are dithiobenzoates, trithiocarbonates, dithiocarbamates, and xanthates. The R group represents the new radical species that will add monomers and grow the polymeric chain. To ensure efficient initiation, the R group should be preferentially formed over the propagating radical, allowing all small molecule CTA to be converted to polymeric CTA. The Z group is responsible for stabilizing the intermediate radical, ensuring efficient addition of the radical to the CTA and efficient fragmentation. Dithiobenzoates are the most stabilizing Z group as they contain a highly conjugated phenyl Z group in contrast to xanthates, which are among the least stabilizing as they contain an alkoxy group which provides poor resonance stabilization of the intermediate radical.

A phenomenon in radical polymerization is rate retardation, which can cause the reaction rate in many RAFT polymerizations to be measurably lower when higher concentrations of CTA are employed. Ideally, the chain transfer reaction has no bearing on the total radical concentration and associated polymerization rate, as the RAFT equilibrium does not create nor consume radicals.<sup>10,11</sup> Experimentally, however this is not always the case, with certain RAFT systems showing substantially reduced rates with higher CTA concentrations.<sup>12</sup> Although small decreases in polymerization rate can be anticipated in RAFT, since smaller growing chains lead to higher termination rate coefficients, this alone is insufficient to rationalize the observed decrease in polymerization rate at higher CTA loadings.<sup>7</sup> Several explanations have been given including cross termination of intermediate radicals with propagating radicals, slow re-initiation, slow fragmentation of the intermediate radicals in one or both equilibria, or a complex combinations of these concepts.<sup>4</sup> Rate retardation within the RAFT main equilibrium has received significant interest for dithiobenzoate CTA.<sup>13</sup> Rate retardation has been studied using the dithiobenzoate CTA in systems which use methyl acrylate,<sup>14</sup> styrene,<sup>15,16</sup> *n*-butyl acrylate,<sup>17</sup> methyl methacrylate,<sup>15,18</sup> and *tert*-butyldimethylsilyl methacrylate.<sup>19</sup>

Moad and team elicited many ‘avoidable causes’ such as oxygen presence, impurities, non-ideal solvents, and poor choices

of R and Z groups of CTA that could lead to rate retardation in RAFT polymerization.<sup>20</sup> In order to mitigate these causes of rate retardation, well-suited conditions were used to conduct these different monomer class systems. Perrier and coworkers highlight that dithiobenzoates were ideal for 1,1-disubstituted more active monomers (MAMs), such as methyl methacrylate (MMA), although tend to show rate retardation for systems with monosubstituted MAMs or less active monomers, (LAMs).<sup>21</sup> Perrier notes that xanthates were ideal CTAs for vinyl acetate (VA).<sup>10</sup> Thang and Moad showed that trithiocarbonates are excellent CTAs for a variety of MAMs; which include styrene (Sty) and methyl acrylate (MA).<sup>22</sup> Well-suited systems of matched monomer and CTA are seen in Scheme 2.

Monomer				
Chain Transfer Agent				

**Scheme 2:** Matched monomer and CTA systems.

We herein investigate rate retardation as it applies to systems beyond traditional dithiobenzoates and explore the possible universality of rate retardation in RAFT. In moving beyond dithiobenzoates, two of the several models found in the literature<sup>13</sup> are used to represent the results, the slow fragmentation model (SFM)<sup>23,24</sup> and intermediate radical termination (IRT)<sup>25,26</sup> model. Using simple scaling law analysis in the IRT and SFM, rate retardation is found to be a universal phenomenon, capable of being explained by a single function, and primarily dictated by the RAFT equilibrium constant. Monomer/CTA combinations with higher equilibrium constants for the formation of the intermediate also have stronger retardation, following a single function.

## RESULTS AND DISCUSSION

The main objective of the current work is to investigate the universality of rate retardation in RAFT across a variety of monomer and CTA activity levels. Many reported systems change the radical initiator concentration in proportion to CTA concentration in order to obtain a desired number of living chains, however, the concurrent variation of CTA and initiator concentrations can obscure retardation effects. Our systems do not vary in initiator concentration, rather only changing the concentration of CTA added to each system, to keep the rate of radical generation by decomposition of AIBN constant throughout the experiments. Initially, rate retardation was investigated for a range of monomers, MMA, Sty, MA, and VA, under well-suited conditions, as reported in the literature.<sup>10,21,22</sup> Temperatures commonly used with polymerization of VA and MA occurred around 60°C.<sup>27,28</sup> Temperature for Sty polymerization was reported between 60-80 °C with temperatures not to exceed 100°C to prevent spontaneous thermal initiation,<sup>29</sup> which could complicate kinetic analysis. Temperatures for ideal MMA polymerization were shown between 60-90°C in the literature.<sup>28</sup> As increasing temperature increases reaction rates and reduces rate retardation effects, here, the temperature for each monomer type was held constant to allow for only variations in rate to be exhibited by the concentration of CTA. Extreme temperature

were excluded as they could potentially decompose the CTA<sup>30</sup> and cause thermolysis of the end group.<sup>31</sup> Our approach will elucidate whether or not retardation can be considered a general feature of well-controlled RAFT polymerization, even outside the standard dithiobenzoate CTAs which are most frequently considered in this context.<sup>7,17,32–35</sup> Polymerizations were performed using monomer to CTA ratios of 100:0.3, 100:1, or 100:3.

Initially, a dithiobenzoate CTA was employed with MMA polymerization, a disubstituted MAM, which should be a well-matched system. Figure 1A shows the kinetic data for the polymerization of MMA in DMSO at 70 °C with an MMA:AIBN ratio of 100:0.2, with varying amounts of 2-cyano-2-propyl benzodithioate (CPDB) as the CTA. As seen in Figure 1A, the rate of polymerization decreases notably with higher CTA loadings at constant radical initiator, consistent with the general phenomenon of rate retardation in RAFT. These retardation effects have been extensively studied on monosubstituted monomers such as Sty and MA using dithiobenzoate CTAs,<sup>14–16</sup> however disubstituted MAMs have received limited attention with evidence of retardation being limited mainly to after gelation,<sup>18</sup> systems with different combinations of initiator and CTA,<sup>15</sup> or to those with limited retardation beyond an induction period as was observed in *tert*-butyldimethylsilyl methacrylate.<sup>19</sup> The data in Figure 1A clearly indicate that retardation effects extend to disubstituted monomers and dithiobenzoates such as MMA with CPDB at 70 °C. None of the reactions exhibited signs of an induction period. However - and such a phenomenon can be observed in several of the data sets included in our study - the first order plots are not strictly linear, but suggest an increase in rate as a function of time to the point where outright initial inhibition is initially observed. We note that neither the simple SFM model nor the IRT model can represent the observed conversion time data, and emphasize that the current study does not address model adequacy or validity. The two models are employed to rationalize the generality of retardation phenomena. Further, experimental uncertainties up to 5% in conversion especially at lower signal to noise results in higher conversion,<sup>36</sup> must be taken into consideration at each timepoint due to conversions being estimated by NMR spectroscopy, which could affect the kinetic analysis. As seen in Figure 1B, the  $M_n$  was relatively close to theory for the 100:0.3 and 100:1 systems and the dispersities for these systems were in the order of 1.25. Figure 1B shows that the 100:3 system provided a lower  $M_n$  value and a dispersity around 1.4-1.5. As expected, retardation did not compromise the ability of the CTA to control the polymer growth, with the more strongly retarded systems had better controlled polymers.

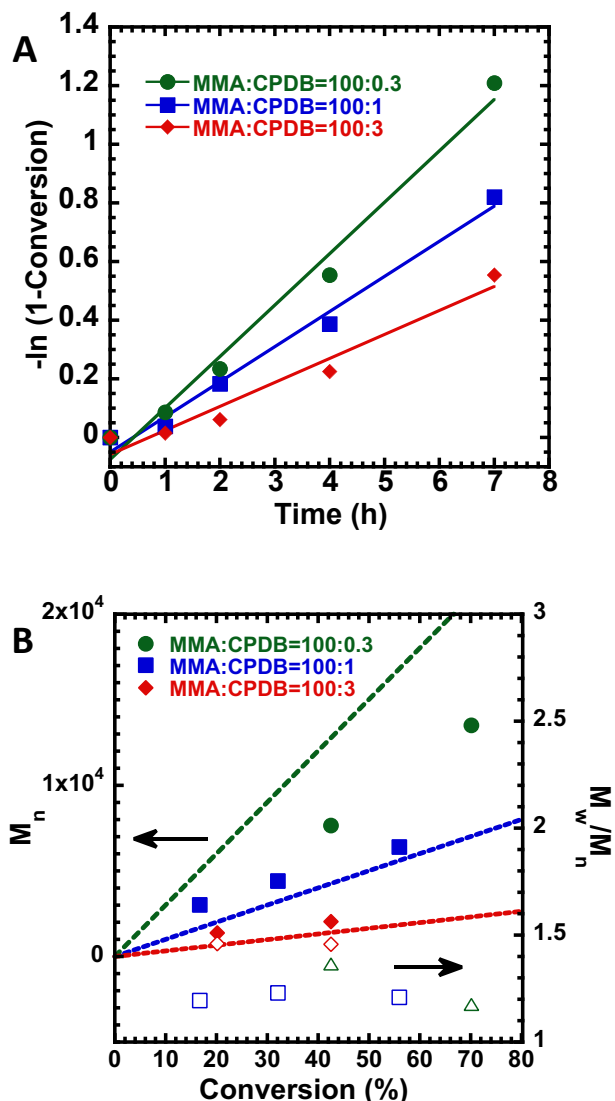


**Figure 1.** Kinetic data for PMMA synthesis showing the plots of (A) the conversion over time with linear slope and (B) the obtained  $M_n$  (solid points), theoretical  $M_n$  (dashed lines) and dispersity (hollow points) vs conversion. Reactions were run at 70 °C under the following conditions: [MMA]:[CPDB]:[AIBN] = 100:0.3:0.2, 100:1:0.2, and 100:3:0.2.

Figure 2A shows the kinetic data for the polymerization of VA in DMSO at 55 °C with a VA:AIBN ratio of 100:0.5 equivalents of AIBN and varying amounts of 2-(ethoxycarbonothioyl)sulfanyl propanoic acid (EtPAX) CTA. VA is a LAM, requiring either a xanthate or dithiocarbamate CTA to encourage fragmentation of the growing radical chain and delocalize charge onto the sulfur of the CTA.<sup>27</sup> Use of withdrawing Z groups with VA polymerization have been known to cause retardation effect,<sup>37</sup> but even xanthates can cause some decreases in polymerization rate both through induction periods and in the steady state.<sup>27</sup> Since a xanthate is among the least active CTAs, using VA with a xanthate is an excellent way of testing the universality of retardation.

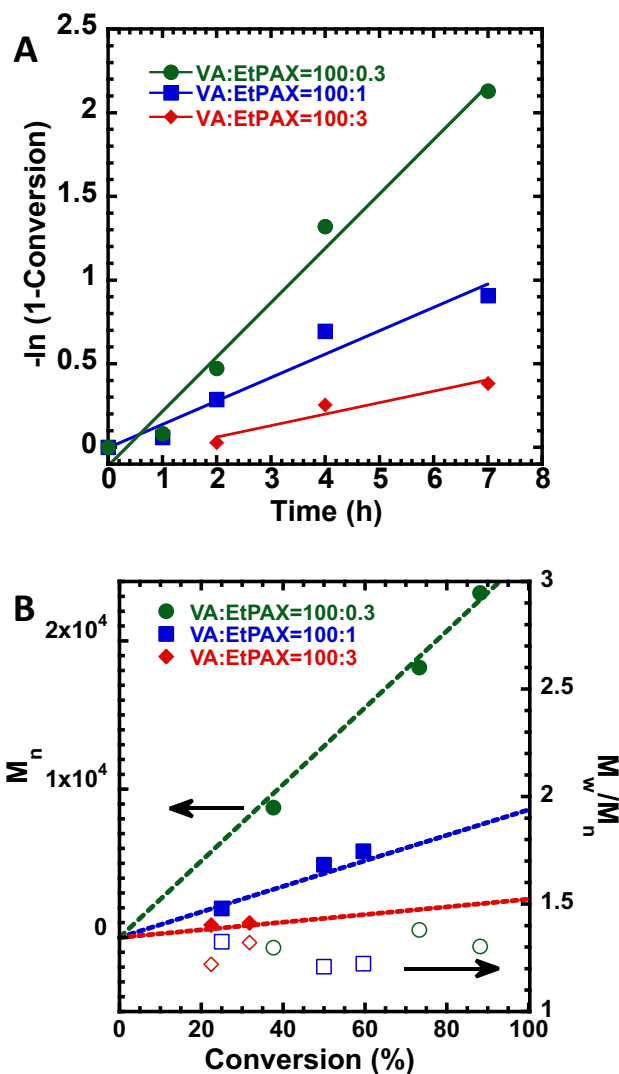


**Figure 2.** Kinetic data for PVA synthesis showing the plots of (A) the conversion over time with linear slope and (B) the obtained  $M_n$  (solid points), theoretical  $M_n$  (dashed lines) and dispersity (hollow points) vs conversion. Reactions were run at 55°C under the following conditions: [VA]:[EtPAX]:[AIBN] = 100:0.3:0.5, 100:1:0.5, and 100:3:0.5.

Figure 2A shows that increasing the amount of EtPAX in VA systems drastically decreases the rate of polymerization. This clearly shows that even while using one of the least active CTAs, retardation occurs, at least for the polymerization of the LAM, VA. The reaction containing 3 equivalents of EtPAX showed an induction period close to two hours, which was accounted for when determining the apparent rate of polymerization and steady state radical concentration in the IRT model. An induction period for VA polymerization is well documented due to the pre-equilibrium step in the RAFT mechanism; this occurs as no polymerization can take place until the original RAFT agent has been transformed to the vinyl ester monoadduct.<sup>38</sup> As seen in Figure 2B, the  $M_n$  values increased linearly with conversion for each CTA concentration, with dispersity values in the range of 1.2-1.3 across all systems.

In the polymerization of monosubstituted MAMs, trithiocarbonates have been suggested as optimal CTAs, reducing the extent of rate retardation by R and Z group reactivity matching.<sup>15</sup> Therefore, two monosubstituted MAM; i.e. MA and Sty, were polymerized in the presence of dodecylthiocarbonylthio-2-methylpropanoic acid (IBADTC) as the CTA. Figure 3A displays the kinetic data for the polymerization of MA in DMSO at 60°C with a MA:AIBN ratio of 100:0.2 equivalents AIBN and varying amounts of IBADTC.

Similarly, to the MMA and VA systems, Figure 3A shows that increasing the amount of IBADTC in MA systems decreases the rate of polymerization. The reaction containing 3 equivalents of IBADTC exhibited an induction period of 1-2 hours, which was considered when evaluating apparent polymerization rates and radical concentrations using the IRT model. As indicated in Figure 3B,  $M_n$  values increased linearly with conversion for each of the varying CTA concentrations and the dispersity remained consistently around 1.1-1.15.

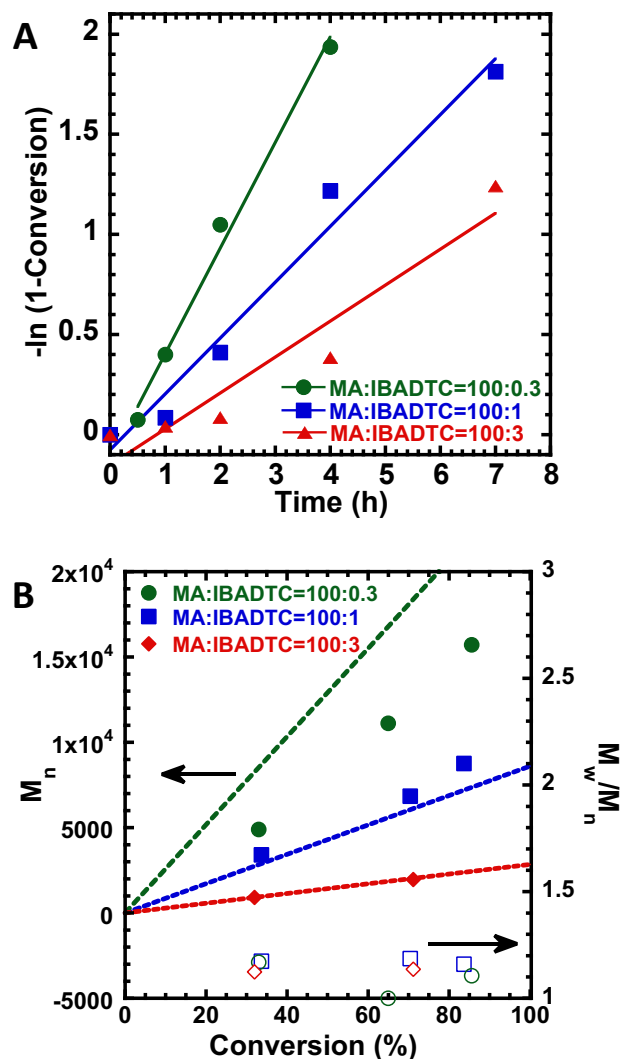


**Figure 3.** Kinetic data for PMA synthesis showing the plots of (A) the conversion over time with linear slope and (B) the

obtained  $M_n$  (solid points), theoretical  $M_n$  (dashed lines) and dispersity (hollow points) vs conversion. Reactions were run at 60°C under the following conditions: [MA]:[IBADTC]:[AIBN] = 100:0.3:0.2, 100:1:0.2, and 100:3:0.2.

Finally, the relatively stabilized monofunctional monomer Sty was evaluated for retardation with trithiocarbonates. Figure 4A displays the kinetic data for the polymerization of Sty in bulk at 65 °C with ratios of Sty:AIBN of 100:0.2 and varying amounts of IBADTC. Figure 4A indicates that styrene exhibits less rate retardation than MA with the same CTA because the Sty monomer is more stable than acrylates due to resonance stabilization through the aromatic ring. Weak rate retardation was observed when comparing polymerization with Sty:IBADTC ratios of 100:0.3 and 100:1, requiring even high loadings of the CTA. Mild retardation was observed when comparing the polymerizations with Sty:IBADTC ratios of 100:1 and 100:3. Therefore, even the highly resonance stabilized monomer is subject to retardation when polymerized in the presence of a well-suited CTA such as IBADTC. All reactions showed signs of an induction period, albeit longer induction times for reactions with increased CTA concentration, which was accounted for when calculating steady state apparent polymerization rates and radical concentrations. Induction periods can be explained due to radical transition from 3° to 2° in the chain equilibrium step. Figure 4B shows that  $M_n$  values were comparable, albeit slightly higher than theory while the dispersities were consistently in the order of 1.1-1.2.

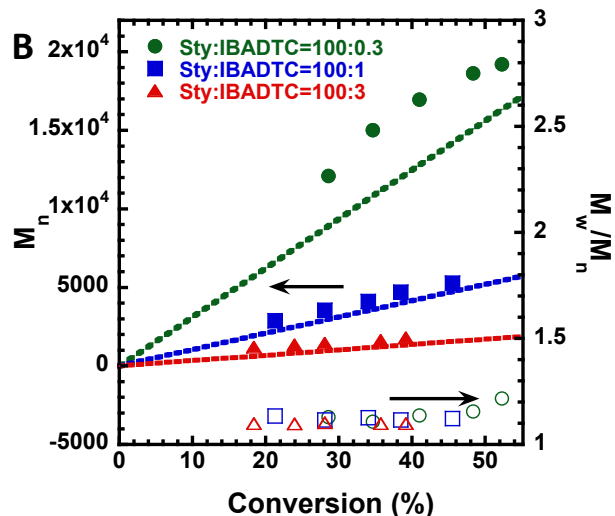
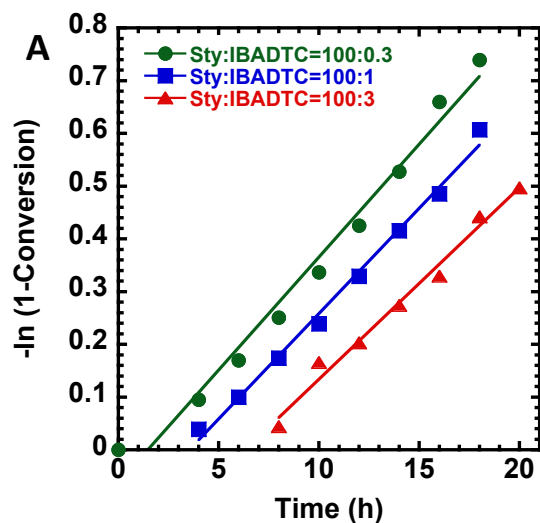
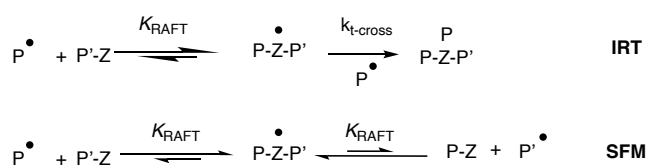


**Figure 4.** Kinetic data for PSty synthesis showing the plots of (A) the conversion over time with linear slope and (B) the obtained  $M_n$  (solid points), theoretical  $M_n$  (dashed lines) and dispersity (hollow points) vs conversion. Reactions were run at 65°C under the following conditions: [Sty]:[IBADTC]:[AIBN] = 100:0.3:0.2, 100:1:0.2, and 100:3:0.2.

The data in Figures 1-4 clearly suggest that retardation is likely to be a consequence of control in RAFT polymerization, even while using well suited CTAs, implying that the formation of the intermediate radical is connected with the observed retardation phenomenon across a diverse range of CTAs with distinct Z groups. Although some decrease in conversion could be explained due to slow addition of the R group to the monomer. However, all cases displayed measurable decreases in polymerization rate with increased CTA loading, even after initial periods of no or very slowly increasing polymerization rates. It appears that the missing step model,<sup>39</sup> which requires a benzene ring on the Z group, is unlikely to explain the rate retardation found in the MA, VA, and styrene systems, shown in Figures 2-4, as they do not use a dithiobenzoate CTA. Instead, the two standard models in their simplest form, IRT and SFM, are used in further analysis of the kinetic data, as seen in Scheme 3.



**Scheme 3:** Top intermediate radical termination (IRT) model and bottom slow fragmentation model (SFM).

In addition to the 4 kinetic data sets shown in Figures 1-4, additional polymerization data were used to evaluate the universality of rate retardation in RAFT. MMA polymerization with a cumyl dithiobenzoate (CDB) from Chong et al.,<sup>15</sup> Sty polymerization with CPDB from Konkolewicz et al.,<sup>7</sup> and MA

polymerization with 1-phenylethyl dithiobenzoate (PEDB) from Perrier et al.,<sup>33</sup> all performed at 60 °C, and MA polymerization with CDB from Drache et al.<sup>35</sup> performed at 80°C are considered. For each system the AIBN dissociation rate,  $k_d$ , is estimated using parameters reported by Moad,<sup>40</sup> with initiator efficiencies taken to be 0.65 for each system. Sty,<sup>41</sup> MA,<sup>42</sup> MMA,<sup>43</sup> and VA<sup>44</sup> propagation rate coefficients are determined at each temperature using parameters in the literature.

In the case of the IRT model, the average radical concentration in the retarded system,  $[P^\cdot]$ , can be compared to the unretarded, or conventional radical polymerization system,  $[P^\cdot]_0$ . In estimating  $[P^\cdot]_0$  a constant, or non-chain-length dependent termination rate coefficient ( $k_t$ ) was used, which averages  $k_t$  over all chain lengths. Since the focus of this work is scaling and trend analysis, a full chain length dependent  $k_t$  analysis would be outside the level of theory used in this analysis. As shown in the supporting information a scaling law for  $[P^\cdot]$  relative to  $[P^\cdot]_0$  can be derived in terms of the RAFT equilibrium constant,  $K_{RAFT}$ , and the CTA concentration.

$$\frac{[P^\cdot]}{[P^\cdot]_0} = \frac{1}{(1 + K_{RAFT}[CTA])^{1/2}} \quad (1)$$

Note that  $[P^\cdot]$  is estimated from a linear fit to a given kinetic experiment's semilogarithmic plot, representing the average radical concentration across the polymerization. The scaling law in Eq 1 applies in the main RAFT equilibrium, after all small molecule CTA is converted to polymeric CTA, comparing the steady state polymerization  $[P^\cdot]$  in the RAFT system to that of conventional radical polymerization  $[P^\cdot]_0$ .

Eq 1 leads to a  $-1/2$  order of steady state radical concentration with  $K_{RAFT}$  and also  $[CTA]$ , once  $K_{RAFT}[CTA]$  is much larger than unity. As seen in Figure 5A, the fit of the IRT model to retarded kinetic experiments across a range of CTAs and monomers is excellent. The eight CTA-monomer pairs and over 24 kinetic experiments were collapsed onto the scaling law of Eq 1. Parameters used to fit the data are given in Table S1 and full experimental data is given in Figures S2-S9. Note all chain length averaged termination rate coefficients,  $k_t$ , were in the order of high  $10^7$ - $10^8$   $M^{-1}s^{-1}$  as is typical for polymeric systems.<sup>45</sup> The sum of differences between the IRT model and experiment defined as  $\chi^2$  values of Eq S25 across the 4 decades in parameters of  $K_{RAFT}$  and  $k_t$  was evaluated, relative to the fit using the parameters in Table S1. In the IRT analysis, this variation in the fit or  $\chi^2$  values are given in Figures S10-S17. In most cases clearly defined minima in the  $\chi^2$  were obtained. The exceptions were strongly retarded systems, where there was an inverse correlation of  $k_t$  and  $K_{RAFT}$ . This inverse correlation can be predicted from Eq 1, since strongly retarded systems will have  $K_{RAFT}[CTA] \gg 1$ , and since  $[P^\cdot]_0 \propto k_t^{-0.5}$ . Despite this apparent lack of certainty over the parameters, confidence in the estimates in Table S1 can be gained by noting that the estimated values of  $k_t$  were in the order of high  $10^7$ - $10^8$   $M^{-1}s^{-1}$  consistent with termination kinetics of macroradicals in solution.<sup>45</sup>

Similarly, a scaling approximation analysis can be carried out in the SFM model. Since the SFM is a non-steady state model, it is not possible to consider an average radical concentration.

However, a scaling law has been developed for the radical concentration at time  $t$ ,  $[P^\cdot]$ , compared to that of a system without any retardation,  $[P^\cdot]_0$ , as seen below:

$$\frac{[P^\cdot]}{[P^\cdot]_0} = \tanh\left(\frac{[P^\cdot]_0 k_t t}{K_{RAFT}[CTA]}\right) \quad (2)$$

Here  $\tanh$  is the hyperbolic tangent function. Note as is typical in a pure SFM model, at sufficiently long time, the intermediate radical builds up and no further retardation would be predicted. This approximate relationship was validated against a full kinetic simulation in Figure S1, showing good agreement between the approximate law in Eq 1 and typical SFM RAFT polymerization with various CTA loadings.

As seen in Figure 5B, the experimentally determined radical concentration, determined using the slope between two adjacent kinetic timepoints – which is beset with a considerable error – follows the trend predicted by the SFM model with fitted values of  $K_{RAFT}$  for each monomer-CTA pair at a given temperature. The larger density of datapoints in Figure 5B, compared to Figure 5A, is due to the non-steady state nature of the SFM, implying that each timepoint must be considered. However, the same kinetic experiments were considered in both the SFM and IRT. The sum of differences between the SFM model and experiment defined as  $\chi^2$  values of Eq S27 across the 4 decades in parameters of  $K_{RAFT}$  and  $k_t$  was evaluated, relative to the fit using the parameters in Table S1. The variation in the  $\chi^2$  values for the SFM model is shown in Figures S18-S25. In most cases a clear minimum is observed, except in strongly retarded systems. Within the SFM framework, strong retardation implies almost exclusive formation of the intermediate radical, greatly suppressing the impact of termination and therefore the impact of  $k_t$  on the fit to the data.

In both Figure 5A and 5B, higher  $K_{RAFT}$  values led to substantially stronger retardation, as a higher  $K_{RAFT}$  leads to a higher intermediate radical concentration, causing more cross termination in the IRT model or an accumulation of non-propagating radical species in SFM. The IRT model appears to have a closer fit to the overall data, although, the discrepancy in Figure 5B could stem from the increased experimental uncertainty associated with analyzing each data point individually (see above). The data in Figure 5B show that the SFM analysis gives essentially as many points above and below the predicted model function, albeit with the larger variability than those in Figure 5A and IRT analysis. The IRT analysis of Figure 5A shows the data can be successfully mapped to the scaling law, showing the transition between a regime of essentially no retardation to a regime where the radical concentration scales as the  $-0.5$  power of  $K_{RAFT}[CTA]$  as the product of  $K_{RAFT}[CTA]$  is increased. The SFM analysis of Figure 5B also shows the correct behavior as the product of  $t(K_{RAFT}[CTA])^{-1}$  increases, leading to less retardation at higher values of  $t(K_{RAFT}[CTA])^{-1}$ , albeit the transition is less clearly seen in the data due to the larger variability of the data points.

As seen in Figure S26, when using  $K_{RAFT}$  values of between  $10^1$ - $10^5$ , consistent with the IRT analysis of Table S1, the



intermediate radical concentrations are in the order of high nanomolar to micromolar for typical propagating radical concentration. In contrast, when using  $K_{\text{RAFT}}$  values consistent with SFM analysis of  $10^5$ - $10^8$  of Table S1, millimolar intermediate radical concentrations are predicted. On the other hand, the IRT predicts very high concentrations of intermediate termination product. It is important to note that EPR experiments in the literature are generally consistent with the high nanomolar to micromolar concentrations of intermediate radical, predicted by the IRT model, although time resolved EPR experiments can show slow fragmentation rates.<sup>13,46,47</sup> The IRT model predicts high concentrations of 3 arm star polymers (Figure S27), as the main termination product, although the experimental data do not support such high concentrations.<sup>48</sup>

Regardless, the data in Figure 5 collectively show that retardation in RAFT is a universal phenomenon, and that all retardation systems can be explained using a single scaling law, which is distinct for each model, with the CTA concentration and the  $K_{\text{RAFT}}$  for the monomer-CTA pair dictating the extent of retardation. In particular, stronger retardation is observed for less stabilized monomers such as acrylates, especially with more stabilizing CTAs such as dithiobenzoates, but even with less stabilizing trithiocarbonates. However, even more stabilized monomers such as MMA or Sty are still subjected to the same retardation features, although Sty with a trithiocarbonate CTA requires very high CTA concentrations (near 0.5M) to exhibit appreciable retardation. Further, even some of the least active CTAs such as xanthates lead to substantial retardation of LAMs such as VA. Notably, due to higher fragmentation rates at elevated temperatures,<sup>49</sup> retardation decreased with higher temperatures, since MA polymerization mediated by dithiobenzoate CTAs showed close to a factor of 5 decrease going from the data at 60 °C of Perrier et al.<sup>33</sup> to 80 °C of Drache et al.<sup>35</sup> as seen in Figure 5 and Table S1.

It is noteworthy that the universality of retardation in RAFT polymerization requires consideration in other contexts. For instance, to access the chain length dependence of termination (CLD-T) rate coefficients, distinct concentrations of CTA were used in RAFT-CLD-T studies. The current study highlights that the choice of RAFT agent – as noted in the respective studies<sup>50,51</sup> – is critical, as a poor choice of CTA concentration can lead to an overestimation of the overall magnitude of the termination rate coefficient.<sup>52</sup>

Beyond the studies described above there is evidence in literature for retardation, even under well-suited RAFT conditions. For example, the steady state bulk polymerization rate of MA was unaffected when the AIBN and trithiocarbonate CTA were increased in the same ratio, indicating that the higher radical concentration from the higher AIBN loading was completely offset by the stronger retardation from the higher CTA loading as predicted by Eq 1.<sup>53</sup> A similar phenomenon has also been observed in a photoinduced electron/energy transfer-RAFT, with a  $-1/2$  order of polymerization rate with CTA loading observed when MA was polymerized with trithiocarbonate CTAs, which is consistent with strongly retarded law predicted in Eq 1.<sup>54</sup>

The results from this analysis indicate that even highly efficient monomer-CTA pairings are typically strongly affected by retardation in RAFT. Indeed, control in RAFT polymerization requires the formation of the intermediate radical at a rate comparable or faster than propagation. Therefore, the necessary formation of the intermediate radical also causes a depression of RAFT polymerization rate, with stronger retardation caused by higher activity CTAs with larger  $K_{\text{RAFT}}$  values. The analysis also indicates that very high loadings of CTA will increase retardation effects, suggesting that retardation may be very strong for systems such as single unit monomer insertion experiments (SUMI).<sup>55,56</sup>

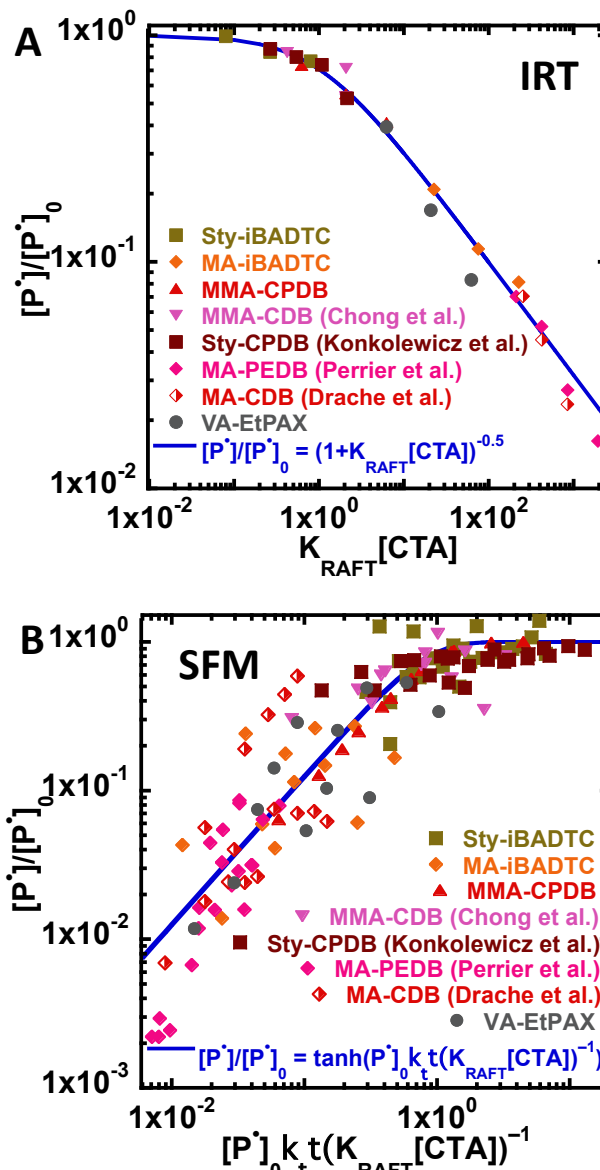


**Figure 5.** Comparison of experimental and scaling law predictions for a range of monomer-CTA pairs. A) Compares the reduction in steady state radical concentration with the scaling law predicted from the IRT model, B) gives the reduction in radical concentration at each kinetic timepoint with the scaling law predicted from the SFM.

## CONCLUSION

We herein demonstrate that rate retardation was seen in all well suited systems, irrespective of CTA classification. Rate retardation does not only occur with dithiobenzoate CTAs, but also with xanthates and trithiocarbonates making this a universal phenomenon amongst all RAFT polymerizations systems. The kinetic data for all systems were analyzed using both the slow fragmentation and intermediate radical termination models. The results suggest – irrespective of the model applied – that rate retardation can be scaled using simple relationships across a variety of monomers and CTAs.

## ASSOCIATED CONTENT

Experimental procedures, supplementary figures and calculations. This material is available free of charge via the Internet at <http://pubs.acs.org>.

## AUTHOR INFORMATION

### Corresponding Author

**Dominik Konkolewicz**- Department of Chemistry and Biochemistry, Miami University, Oxford, OH, 45056, United States. Email: [d.konkolewicz@miamioh.edu](mailto:d.konkolewicz@miamioh.edu)

**Athina Anastasaki**- Laboratory of Polymeric Materials, Department of Materials, ETH Zurich, Vladimir-Prelog-Weg 5, Zurich, Switzerland. Email: [athina.anastasakis@mat.ethz.ch](mailto:athina.anastasakis@mat.ethz.ch)

**Christopher Barner-Kowollik**- Centre for Materials Science, School of Chemistry and Physics, Queensland University of Technology (QUT), 2 George Street, Brisbane, Queensland 4000, Australia. Email: [christopher.barnerkowollik@qut.edu.au](mailto:christopher.barnerkowollik@qut.edu.au)

### Notes

The authors declare no competing financial interest.

## ACKNOWLEDGMENTS

This work was partially supported by the National Science Foundation under Grant No. (DMR- 1749730) to D.K for supporting polymerization experiments and scaling law development. 400 MHz NMR instrumentation at Miami University is supported through funding from the National Science Foundation under grant number (CHE- 1919850). D.K. acknowledges equipment support from Miami University through startup funding and the Robert H. and Nancy J. Blayney Professorship. A.A. gratefully acknowledges ETH Zurich for aid in designing reaction conditions. C.B.-K. acknowledges the Australian Research Council (ARC) for funding to aid kinetic analysis in the context of a Laureate Fellowship as well as the Queensland University of Technology (QUT) for continued support, including through its Centre for Materials Science.

## REFERENCES

- (1) Parkatzidis, K.; Wang, H. S.; Truong, N. P.; Anastasaki, A. Recent Developments and Future Challenges in Controlled Radical Polymerization: A 2020 Update. *Chem* **2020**, *6* (7), 1575–1588.
- (2) Zhang, K.; Monteiro, M. J.; Jia, Z. Stable Organic Radical Polymers: Synthesis and Applications. *Polym. Chem.* **2016**, *7*, 5589–5614.
- (3) Corrigan, N.; Jung, K.; Moad, G.; Hawker, C. J.; Matyjaszewski, K.; Boyer, C. Reversible-Deactivation Radical Polymerization (Controlled/Living Radical Polymerization): From Discovery to Materials Design and Applications. *Prog. Polym. Sci.* **2020**, *111*, 101311.
- (4) Keddie, D. J.; Moad, G.; Rizzardo, E.; Thang, S. H. RAFT Agent Design and Synthesis. *Macromolecules* **2012**, *45*, 5321–5342.
- (5) Gregory, A.; Stenzel, M. Complex Polymer Architectures via RAFT Polymerization: From Fundamental Process to Extending the Scope Using Click Chemistry and Nature's Building Blocks. *Prog. Polym. Sci.* **2012**, *37* (1), 38–105.
- (6) Tobita, H. Molecular Weight Distribution of Living Radical Polymers. *Macromol. Theory Simulations* **2006**, *15* (1), 12–22.
- (7) Konkolewicz, D.; Hawket, B. S.; Gray-weale, A.; Perrier, S. RAFT Polymerization Kinetics: Combination of Apparently Conflicting Models. *Macromolecules* **2008**, *41*, 6400–6412.
- (8) Harrisson, S. The Chain Length Distribution of an Ideal Reversible Deactivation Radical Polymerization. *Polymers* **2018**, *10* (8).
- (9) Konkolewicz, D.; Siau, M.; Gray-Weale, A.; Hawket, B. S.; Perrier, S. Obtaining Kinetic Information from the Chain-Length Distribution of Polymers Produced by RAFT. *J. Phys. Chem. B* **2009**, *113* (20), 7086–7094.
- (10) Perrier, S.; Takolpuckdee, P. Macromolecular Design via Reversible Addition –. *J. Polym. Sci. Part A Polym. Chem.* **2005**, *43*, 5347–5393.
- (11) Moad, G.; Solomon, D. H. *The Chemistry of Free Radical Polymerization*, 1st ed.; Elsevier: Amsterdam, 1995, 279–325.
- (12) Gao, Y.; Lv, L.; Zou, G.; Zhang, Q. Dependence of Cross-Termination Rate on RAFT Agent Concentration in RAFT Polymerization. *Macromol. Res.* **2017**, *25* (9), 931–935.
- (13) Barner-Kowollik, C.; Buback, M.; Charleux, B.; Coote, M. L.; Drache, M.; Fukuda, T.; Goto, A.; Klumperman, B.; Lowe, A. B.; Mcleary, J. B.; Moad, G.; Monteiro, M. J.; Sanderson, R. D.; Tonge, M. P.; Vana, P.; Marie, P. Mechanism and Kinetics of Dithiobenzoate-Mediated RAFT Polymerization. I. The Current Situation. *J. Polym. Sci. Part A Polym. Chem.* **2006**, *44*, 5809–5831.
- (14) Perrier, S.; Barner-Kowollik, C.; Quinn, J. F.; Vana, P.; Davis, T. P. Origin of Inhibition Effects in the Reversible Addition Fragmentation Chain Transfer (RAFT) Polymerization of Methyl Acrylate. *Macromolecules* **2002**, *35*, 8300–8306.
- (15) Chong, B. Y. K.; Krstina, J.; Le, T. P. T.; Moad, G.; Postma, A.; Rizzardo, E.; Thang, S. H. Thiocarbonylthio Compounds [S=C(Ph)S-R] in Free Radical Polymerization with Reversible Addition-Fragmentation Chain Transfer (RAFT Polymerization). Role of the Free-Radical Leaving Group (R). *Macromolecules* **2003**, *36* (7), 2256–2272.
- (16) Feldermann, A.; Coote, M. L.; Stenzel, M. H.; Davis, T. P.; Barner-Kowollik, C. Consistent Experimental and Theoretical Evidence for Long-Lived Intermediate Radicals in Living Free Radical Polymerization. *J. Am. Chem. Soc.* **2004**, *126* (48), 15915–15923.
- (17) Haven, J. J.; Junkers, T. Mapping Dithiobenzoate-Mediated RAFT Polymerization Products via Online Microreactor / Mass Spectrometry Monitoring. *Polymers* **2018**, No. 10, 1228.
- (18) Peklak, A. D.; Butté, A.; Storti, G.; Morbidelli, M. Gel Effect in the Bulk Reversible Addition-Fragmentation Chain Transfer Polymerization of Methyl Methacrylate: Modeling and Experiments. *J. Polym. Sci. Part A Polym. Chem.* **2006**, *44* (3), 1071–1085.
- (19) Nguyen, M. N.; Margailan, A.; Pham, Q. T.; Bessy, C. RAFT Polymerization of Tert -Butyldimethylsilyl Methacrylate: Kinetic Study and Determination Of. *Polymers* **2018**, *10* (2), 224.
- (20) Moad, G. Mechanism and Kinetics of Dithiobenzoate-Mediated RAFT Polymerization – Status of the Dilemma. *Macromol. Chem. Phys.* **2014**, *215* (1), 9–26.



- (21) Perrier, S. 50th Anniversary Perspective : RAFT Polymerization - A User Guide. *Macromolecules* **2017**, *50*, 7433–7447.
- (22) Mayadunne, R. T. A.; Rizzardo, E.; Chiefari, J.; Krstina, J.; Moad, G.; Postma, A.; Thang, S. H. Living Polymers by the Use of Trithiocarbonates as Reversible Addition-Fragmentation Chain Transfer (RAFT) Agents: ABA Triblock Copolymers by Radical Polymerization in Two Steps. *Macromolecules* **2000**, *33* (2), 243–245.
- (23) Barner-Kowollik, C.; Quinn, J. F.; Morsley, D. R.; Davis, T. P. Modeling the Reversible Addition – Fragmentation Chain Transfer Process in Cumyl Dithiobenzoate-Mediated Styrene Homopolymerizations: Assessing Rate Coefficients for the Addition – Fragmentation Equilibrium. *J. Polym. Sci. Part A Polym. Chem.* **2001**, *39*, 1353–1365.
- (24) Vana, P.; Davis, T. P.; Barner-Kowollik, C. Kinetic Analysis of Reversible Addition Fragmentation Chain Transfer (RAFT) Polymerizations: Conditions for Inhibition, Retardation, and Optimum Living Polymerization. *Macromol. Theory Simulations* **2002**, *11*, 823–835.
- (25) Monteiro, M. J.; Brouwer, H. De. Intermediate Radical Termination as the Mechanism for Retardation in Reversible Addition - Fragmentation Chain Transfer Polymerization. *Macromolecules* **2001**, *34*, 349–352.
- (26) Kwak, Y.; Goto, A.; Fukuda, T. Rate Retardation in Reversible Addition - Fragmentation Chain Transfer (RAFT) Polymerization: Further Evidence for Cross-Termination Producing 3-Arm Star Chain. *Macromol. Theory Simulations* **2004**, *37*, 1219–1225.
- (27) Stenzel, M. H.; Cummins, L.; Roberts, G. E.; Davis, T. P.; Vana, P.; Barner-Kowollik, C. Xanthate Mediated Living Polymerization of Vinyl Acetate: A Systematic Variation in MADIX/RAFT Agent Structure. *Macromol. Chem. Phys.* **2003**, *204* (9), 1160–1168.
- (28) Moad, G.; Rizzardo, E.; Thang, S. H. Radical Addition-Fragmentation Chemistry in Polymer Synthesis. *Polymer* **2008**, *49* (5), 1079–1131.
- (29) Jung, M. L.; Ok, H. K.; Sang, E. S.; Lee, B. H.; Choe, S. Reversible Addition-Fragmentation Chain Transfer (RAFT) Bulk Polymerization of Styrene: Effect of R-Group Structures of Carboxyl Acid Group Functionalized RAFT Agents. *Macromol. Res.* **2005**, *13* (3), 236–242.
- (30) Moad, G.; Rizzardo, E.; Thang, S. H. Radical Addition - Fragmentation Chemistry in Polymer Synthesis. *Polymer* **2008**, *49* (5), 1079–1131.
- (31) Chong, B.; Moad, A. G.; Rizzardo, B. E.; Skidmore, A. M.; A, S. H. T. Thermolysis of RAFT-Synthesized Poly (Methyl Methacrylate). *Aust. J. Chem.* **2006**, *59*, 755–762.
- (32) Ting, S. R. S.; Davis, T. P.; Zetterlund, P. B. Retardation in RAFT Polymerization: Does Cross-Termination Occur with Short Radicals Only? *Macromolecules* **2011**, *44* (11), 4187–4193.
- (33) Perrier, S.; Barner-Kowollik, C.; Quinn, J. F.; Vana, P.; Davis, T. P. Origin of Inhibition Effects in the Reversible Addition Fragmentation Chain Transfer (RAFT) Polymerization of Methyl Acrylate. *Macromolecules* **2002**, *35* (22), 8300–8306.
- (34) Buback, M.; Vana, P. Mechanism of Dithiobenzoate-Mediated RAFT Polymerization: A Missing Reaction Step. *Macromol. Rapid Commun.* **2006**, *27* (16), 1299–1305.
- (35) Drache, M.; Schmidt-Naake, G.; Buback, M.; Vana, P. Modeling RAFT Polymerization Kinetics via Monte Carlo Methods: Cumyl Dithiobenzoate Mediated Methyl Acrylate Polymerization. *Polymer* **2005**, *46* (19 SPEC. ISS.), 8483–8493.
- (36) Malz, F.; Jancke, H. Validation of Quantitative NMR. *J. Pharm. Biomed. Anal.* **2005**, *38* (5 SPEC. ISS.), 813–823.
- (37) Harrison, S.; Liu, X.; Ollagnier, J. N.; Coutelier, O.; Marty, J. D.; Destarac, M. RAFT Polymerization of Vinyl Esters: Synthesis and Applications. *Polymers* **2014**, *6* (5), 1437–1488.
- (38) Pound, G.; McLeary, J. B.; McKenzie, J. M.; Lange, R. F. M.; Klumperman, B. In-Situ NMR Spectroscopy for Probing the Efficiency of RAFT/MADIX Agents. *Macromolecules* **2006**, *39* (23), 7796–7797.
- (39) Buback, M.; Vana, P. Mechanism of Dithiobenzoate-Mediated RAFT Polymerization: A Missing Reaction Step. *Macromol. Rapid Commun.* **2006**, 1299–1305.
- (40) Moad, G. A Critical Assessment of the Kinetics and Mechanism of Initiation of Radical Polymerization with Commercially Available Dialkyldiazene Initiators. *Prog. Polym. Sci.* **2019**, *88*, 130–188.
- (41) Buback, M.; Gilbert, R. G.; Hutchinson, R. A.; Klumperman, B.; Kuchta, F.-D.; Manders, B. G.; O'Driscoll, K. F.; Russell, G. T.; Schweer, J. Critically Evaluated Rate Coefficients for Free-Radical Polymerization, 1. Propagation Rate Coefficient for Styrene. *Macromol. Chem. Phys.* **1995**, *196*, 3267.
- (42) Buback, M.; Kurz, C. H.; Schmaltz, C.; Chemie, P.; Gottingen, U.; Gottingen, D.-. Pressure Dependence of Propagation Rate Coefficients in Free- Radical Homopolymerizations of Methyl Acrylate and Dodecyl Acrylate. *Macromol. Chem. Phys.* **1998**, *1727*, 1721–1727.
- (43) Beuermann, S.; Buback, M.; Davis, T. I.; Gilbert, R. G.; Hutchinson, R. A.; Friedrich, O.; Gregory, O. Critically Evaluated Rate Coefficients for Free-Radical Polymerization, 2 Propagation Rate Coefficients for Methyl Methacrylate. *Macromol. Chem. Phys.* **2006**, *1560* (1997), 1545–1560.
- (44) Hutchinson, R. A.; Paquet Jr., D. .; McMin, J. H.; Beuermann, S.; Fuller, R. E.; Jackson, C. The Application of Pulsed-Laser Methods for the Determination of Free-Radical Polymerization Rate Coefficients. *DEHEMA Monogr.* **1995**, *131*, 467.
- (45) Johnston-Hall, G.; Monteiro, M. J. Bimolecular Radical Termination: New Perspectives and Insights. *J. Polym. Sci. Part A Polym. Chem.* **2008**, *46*, 3155–3173.
- (46) Meiser, W.; Buback, M.; Sidoruk, A. EPR Investigations into the Kinetics of Trithiocarbonate-Mediated RAFT-Polymerization of Butyl Acrylate. *Macromol. Chem. Phys.* **2013**, *214* (18), 2108–2114.
- (47) Ranieri, K.; Delaittre, G.; Barner-Kowollik, C.; Junkers, T. Direct Access to Dithiobenzoate RAFT Agent Fragmentation Rate Coefficients by ESR Spin-Trapping. *Macromol. Rapid Commun.* **2014**, *35* (23), 2023–2028.
- (48) Feldermann, A.; Ah Toy, A.; Davis, T. P.; Stenzel, M. H.; Barner-Kowollik, C. An In-Depth Analytical Approach to the Mechanism of the RAFT Process in Acrylate Free Radical Polymerizations via Coupled Size Exclusion Chromatography–Electrospray Ionization Mass Spectrometry (SEC–ESI–MS). *Polymer* **2005**, *46*, 8448–8457.
- (49) Barner-Kowollik, C.; Junkers, T. Kinetic and Mechanistic Similarities between Reversible Addition Fragmentation Chain Transfer Intermediate and Acrylate Midchain Radicals. *J. Polym. Sci. Part A Polym. Chem.* **2011**, *49*, 1293–1297.
- (50) Johnston-Hall, G.; Stenzel, M. H.; Davis, T. P.; Barner-Kowollik, C.; Monteiro, M. J. Chain Length Dependent Termination Rate Coefficients of Methyl Methacrylate (MMA) in the Gel Regime: Accessing K<sub>ti</sub> Using Reversible Addition-Fragmentation Chain Transfer (RAFT) Polymerization. *Macromolecules* **2007**, *40* (8), 2730–2736.
- (51) Johnston-Hall, G.; Theis, A.; Monteiro, M. J.; Davis, T. P.; Stenzel, M. H.; Barner-Kowollik, C. Accessing Chain Length Dependent Termination Rate Coefficients of Methyl Methacrylate (MMA) via the Reversible Addition Fragmentation Chain Transfer (RAFT) Process. *Macromol. Chem. Phys.* **2005**, *206* (20), 2047–2053.
- (52) Theis, A.; Feldermann, A.; Charton, N.; Davis, T. P.; Stenzel, M. H.; Barner-Kowollik, C. Living Free Radical Polymerization (RAFT) of Dodecyl Acrylate: Chain Length Dependent Termination, Mid-Chain Radicals and Monomer Reaction Order. *Polymer* **2005**, *46* (18), 6797–6809.
- (53) Wood, M. R.; DunCalf, D. J.; Findlay, P.; Rannard, S. P.; Perrier,

- S. Investigation of the Experimental Factors Affecting the Trithiocarbonate-Mediated RAFT Polymerization of Methyl Acrylate. *Aust. J. Chem.* **2007**, 60 (10), 772–778.
- (54) Kurek, P. N.; Kloster, A. J.; Weaver, K. A.; Manahan, R.; Allegrezza, M. L.; De Alwis Watuthanthrige, N.; Boyer, C.; Reeves, J. A.; Konkolewicz, D. How Do Reaction and Reactor Conditions Affect Photoinduced Electron/Energy Transfer Reversible Addition-Fragmentation Transfer Polymerization? *Ind. Eng. Chem. Res.* **2018**, 57 (12), 4203–4213
- (55) Xu, J.; Fu, C.; Shanmugam, S.; Hawker, C. J.; Moad, G.; Boyer, C. Synthesis of Discrete Oligomers by Sequential PET-RAFT Single-Unit Monomer Insertion. *Angew. Chemie - Int. Ed.* **2017**, 56 (29), 8376–8383.
- (56) Xu, J. Single Unit Monomer Insertion: A Versatile Platform for Molecular Engineering through Radical Addition Reactions and Polymerization. *Macromolecules* **2019**, 52 (23), 9068–9093.

## Table of Contents Entry

